AN EXPERIMENTAL INVESTIGATION OF ROBOTIC SPACEWALKING

FREDRIK REHNMARK, IVAN SPAIN
Lockheed Martin Space Operations
Houston, Texas, USA
frehnmar@ems.jsc.nasa.gov

WILLIAM BLUETHMANN, S. MICHAEL GOZA, ROBERT O. AMBROSE
NASA Johnson Space Center
Houston, Texas, USA

KEN ALDER
Hernandez Engineering
Houston, Texas, USA

NASA's Human Space Flight program depends heavily on spacewalks performed by human astronauts. These Extra-Vehicular Activities (EVAs) are risky, expensive and complex. In collaboration with the Defense Advanced Research Projects Agency (DARPA), NASA is developing a robotic astronaut's assistant called Robonaut that could boost EVA productivity while reducing risk and conserving EVA resources. Robonaut is an anthropomorphic robot equipped with human-like dexterous manipulation and microgravity locomotion capabilities. Robots are proposed as cost-effective, energy-efficient tools supporting humans on extended space missions, riding aboard orbiting spacecraft and transit vehicles en route to Mars, the Moon and other destinations.

Spacewalking is poorly named, as it has little in common with how animals walk on Earth. In order to move about in a microgravity environment, a robot must be able to climb autonomously, using gaits that smoothly manage its momentum and that minimize contact forces while providing for safety in the event of an emergency requiring the system to stop. A one-g robotic mobility test is conducted with Robonaut floating on air-bearing equipment that emulates the dynamics of weightless motion and allows the robot to translate under its own power. Test results are presented for a simplified EVA task.

Keywords: Robonaut, NASA, DARPA, EVA, space.

1. Introduction

Among its many benefits, the International Space Station (ISS) serves as a high-fidelity research platform for long-term space travel. A stunning achievement in orbital assembly, the program highlights NASA's heavy reliance on Extra-Vehicular Activity (EVA) spacewalks to connect services, configure external equipment, conduct contingency repairs and perform routine maintenance. Unfortunately, spacewalks demand much preparation, consume significant crew time and pose a resource bottleneck to processes that depend on them.

Risky, expensive and complex, EVA operations are restricted in both duration and scope by consumables and available manpower. Today, the work is carefully coordinated between two astronauts working an 8-hour EVA day. Future manned missions to the Moon, Mars and beyond will face these EVA resource management problems even more acutely as the need for greatly expanded in-space assembly and servicing capabilities grows.

2. Walking in Space

Astronauts use their legs very differently in space than people do on Earth. Many forms of terrestrial locomotion, such as walking, jumping and rolling, depend on the restoring force of gravity to offset impulsive contact forces and maintain the moving body's proximity to the terrain. A human walking across a flat, horizontal surface exerts both normal and tangential contact forces on it. While the tangential component can lie anywhere in the plane of the surface, the normal component arises from compression and results in a vertical ground reaction force accelerating the moving body away from the surface. In the zero-g environment experienced on orbit, ground reaction forces generated during walking would simply launch the walker off the surface after the first step.

For astronauts moving about under their own power, zero-g locomotion is generally accomplished by translating across strategically placed, load-rated handrails (Fig. 1). Unlike our feet, the human hand can form the force-closure grasps needed to generate impulsive contact forces controlling the trajectory of a climbing astronaut. Accordingly, climbing in zero-g involves mostly arm and hand action while leg motion is kept to a minimum to avoid inadvertently kicking sensitive equipment. Only when the astronaut straps his/her feet side-by-side into a Portable Foot Restraint (PFR), as shown in Fig. 1, can the legs be used effectively for positioning the upper body and reacting forces exerted while working.
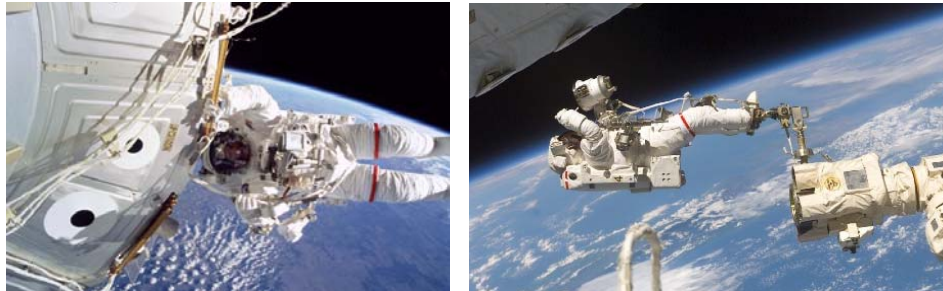

Fig. 1. (left) Climbing using ISS handrails and tethers; (right) Riding on the Space Station RMS in a PFR (Portable Foot Restraint) plugged into a WIF (Worksite InterFace) socket.

Just like terrestrial climbers, spacewalking astronauts connect themselves to their spacecraft using tethers, providing a lifeline in the event they are separated. Every tool that an astronaut is carrying must likewise be tethered to his/her Extra-Vehicular Mobility Unit (EMU) spacesuit. Aboard the ISS, handrails and tether points are distributed along planned translation corridors measuring 43 inches in diameter[1] and branching out all over the facility. Selected EVA worksites are equipped with Worksite Interface (WIF) sockets providing structural attachment points for the PFR. EVA requirements, procedures and timelines are painstakingly developed to ensure safe and ergonomic locomotion during EVA operations.

3. Extra-Vehicular Robotics (EVR)

EVA astronauts are physically limited in both the duration and type of work they can do during a spacewalk. Remote Manipulator System (RMS) class robots can greatly extend the reach and positioning capability of the crew but EVA time is a finite resource governed by consumables. The recent emergence of highly dexterous space robots dramatically expands the opportunities for humans and robots working together in space[2,3]. These machines can help conserve EVA hours by relieving human astronauts of many routine chores and assisting them in more complex tasks. Robots can take risks unacceptable to humans, perform contingency EVA operations in minutes, instead of hours, and setup worksites in preparation for the arrival of human astronauts. An EVA/EVR human-robot team combining the information-gathering and problem-solving skills of human astronauts with the survivability and physical capabilities of space robots is proposed as a strategic pairing designed to increase productivity while reducing risk. Recognizing the opportunity to augment human presence in space with cost-effective machines, the Automation, Robotics and Simulation Division (AR&SD) at NASA's Johnson Space Center (JSC) is collaborating with the Defense Advanced Research Projects Agency (DARPA) to develop a humanoid robot called Robonaut (Fig. 2).
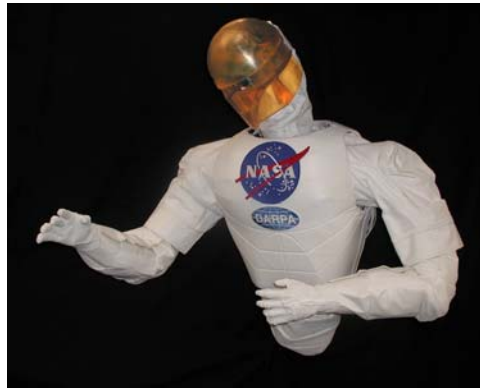

Fig. 2. Ground-based Robonaut testbed.

Unlike other space robots, Robonaut is designed specifically to work with and around humans. The robot's considerable mechanical dexterity allows it to use EVA tools and manipulate flexible materials much like a human astronaut would. About the same size as the EMU spacesuit, Robonaut can go wherever a suited astronaut can. By meeting these requirements, the Robonaut project leverages NASA's enormous investment in tools, procedures, and workspaces for spacewalking astronauts. Although the challenges of designing robots for space and terrestrial applications are very different, a 1-g Robonaut system was built at NASA's Johnson Space Center to develop and test control strategies. A wide array of tools and interfaces have been successfully handled in the course of testing the Robonaut system's capabilities[4].

4. Robonaut System Overview

4.1. *Morphology*

The requirements for interacting with EVA astronauts and their tools in an unstructured environment designed for humans provide the starting point for the Robonaut design[5]. Altogether, the machine incorporates more than 50 coordinated degrees-of-freedom (DOFs) and physical capabilities approaching those of a human in a spacesuit. Anatomically, the robot closely resembles the form of a suited astronaut except that it has only one leg instead of two (Fig. 3). This 7 DOF leg terminates in a latching foot allowing the robot to perch at any EVA worksite equipped with a WIF socket; the same mechanical interface used by the PFR.
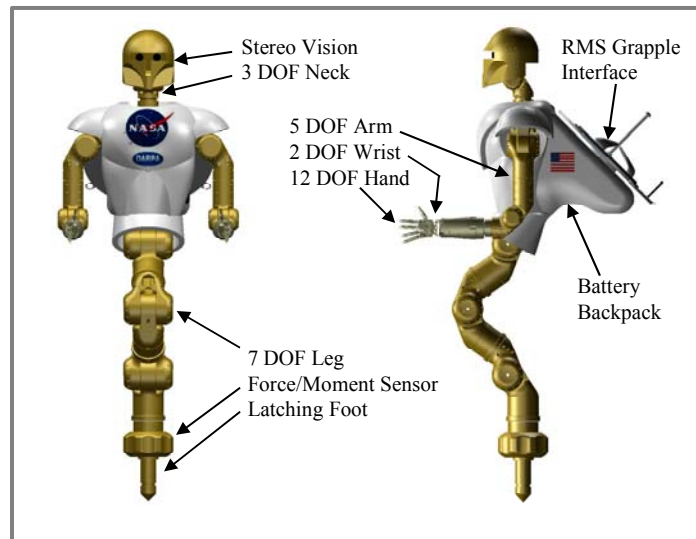
Fig. 3. Anatomy of Robonaut (zero-g configuration).

Once anchored at the worksite, the robot can use its leg to position its upper body within reach of the target task. The anthropomorphic Robonaut design capitalizes on extensive ergonomic analysis of the worksite already performed in configuring it for EVA. Moving between worksites is accomplished by climbing from handrail to handrail, just like a human astronaut. To avoid leaving behind nicks and burrs that could tear an astronaut's spacesuit glove, the robot wears special padded gloves of its own.

4.2. *Command and control*

In its simplest form, Robonaut is a teleoperated master-slave system in which a human teleoperator becomes the robot master. With the exception of the stabilizing leg, the anthropomorphic form of the robot allows an intuitive, one-to-one mapping between master and slave motions. Relative Cartesian position commands are applied in control frames attached to the robot's hands, head and foot and referenced back to the stationary body frame at the center of the chest. Command reindexing allows the teleoperator to maintain a comfortable working posture that minimizes physical fatigue and avoids human reach limits, regardless of the robot's configuration within its workspace. The immersive telepresence interface used in the climbing test is shown in Fig. 4. Because Robonaut is designed to work with and around humans, the human-machine interface is central to the high-level control system design[6], which also incorporates distributed autonomy and learning modules.
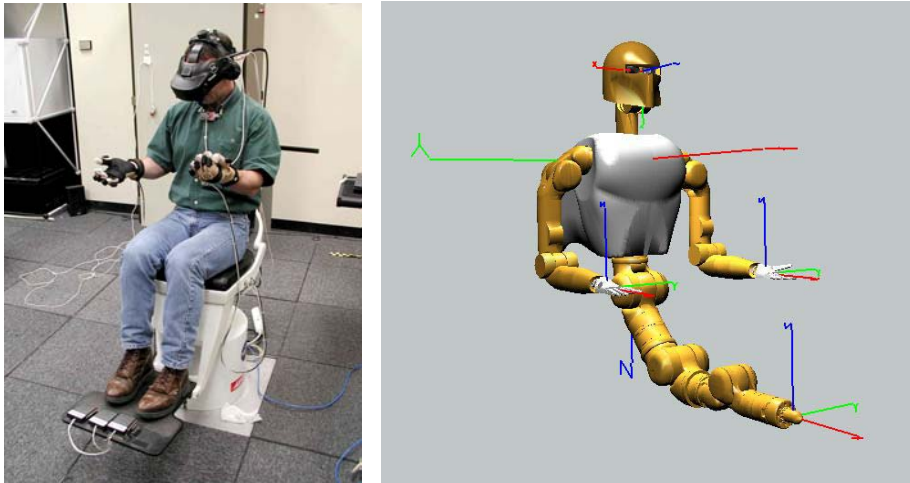

Fig. 4. Cartesian command frames.

The fundamental control methods for Robonaut are Cartesian position control of the arms, neck and leg and joint position control of the hands. A two-tiered force accommodation approach is used to handle external forces. For relatively small forces, Robonaut uses an impedance control law. In this control mode, the arm acts as a mass-spring-damper, complying to external forces, but returning to the original position if the load is relieved. For loads exceeding a user-defined threshold, the arm transitions into a damping control law, where the arm moves at a velocity proportional to the applied load. The two control modes are shown in relation to the rest of the Robonaut arm control laws in Fig. 5.
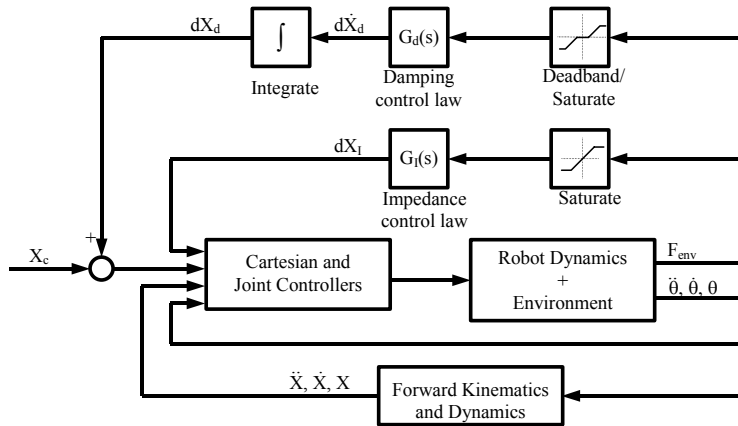
Fig. 5. Robonaut arm control system.

While designed for safety, the force accommodation control laws can also be great tools for performing work. For example, when attempting to place a peg into a hole, the impedance control law may be stiff in the direction of insertion and compliant in the off-axes. This allows the manipulator to apply forces in the insertion direction without building up forces in the other axes.

When interacting with a stiff environment like a spacecraft hull, Robonaut's ability to sense and control interaction forces both protects hardware and allows the robot to work in the presence of hard contact constraints. Force-moment sensors are located near the distal and proximal terminus of each limb, providing sensitive measurements of the interaction between the end-effector and the environment and also detection/localization of contact along the limb in the event of a collision. The control software establishes safety thresholds and will shut down a limb that is exerting excessive force. For the climbing test, a new safety shutdown was developed to reflexively open the hand and release a handrail in response to forces large enough to damage the fingers or wrist. The raw forces measured at the forearm were corrected for the weight of the end-effector using a gravity compensation model and transformed across the wrist pitch and yaw DOFs out to the center of the hand (Fig. 6).
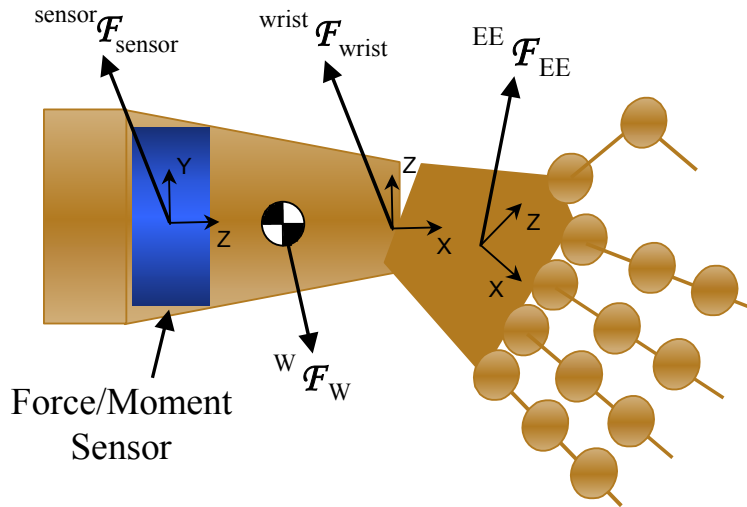
Fig. 6. Force measurement coordinate frames on the Robonaut hand.

4.3. *Zero-g stabilizing leg*

Depending on the nature of the task to be performed, commands to the 7 DOF stabilizing leg (Fig. 7) may come from one of several sources. Because the robot's leg (R-P-R-P-R-P-R) and arms (R-P-R-P-R-P-Y) are kinematically very similar, they can each be teleoperated in the same fashion. By simply redirecting the command stream coming from the human's left or right arm, the leg may be teleoperated effectively to complete coarse positioning and alignment tasks like setting up the foot for automated insertion into a WIF socket. Repeated insertion trials confirmed that the automated insertion algorithm could correct the remaining misalignments and drive the foot into the socket until the latches clicked out, locking the foot into the socket. Finding a useful probe-socket interface camera view for the operator, however, was difficult because the robot's body and arms occluded the view of large regions of the leg's workspace. For this particular task, transitioning to a boresight camera view and a rate-based, instead of position-based, control device would likely improve results considerably.

Fig. 7. The first six distal joints and latching foot of the 7 DOF Robonaut zero-g stabilizing leg.

Force control was required to automatically insert the robot's latching foot completely into the WIF socket. The active component of the insertion command consists of a constant velocity (0.05 in/sec) move along the longitudinal axis of the probe (+x). Force-moment accommodation is implemented to passively improve alignment of the probe with the socket as it makes contact inside the bore. More details of the automated insertion will be discussed in the Results section.

After the foot is securely anchored in the WIF socket, it can serve as a load path supporting the reaction forces and torques required to reposition and stabilize the upper body at a worksite. Internally, the software still sends commands to Robonaut as though the foot is moving, but since the leg is anchored, the body moves instead. With the robot's leg constrained in this way, body-centric position commands are no longer appropriate and the base frame should be relocated to the foot. Likewise, a different strategy is needed to generate leg commands because of the large workspace and non-anthropomorphic motions required. For the purposes of the climbing test, these body-repositioning commands were generated via a rate control GUI by the console operator.

5. Objectives

To validate this new approach to Extra-Vehicular Robotic (EVR) locomotion, a one-g robotic climbing test is conducted. Test objectives include:

- Investigate the challenges of EVR locomotion in micro-g using existing technology prototypes and one-g test beds.
- Demonstrate the feasibility of robotic translation between EVA worksites using standard ISS handrails.
- Demonstrate the feasibility of robotic repositioning at an EVA worksite using a dexterous stabilizing leg compatible with the WIF socket designed for the PFR.
- Develop controllers allowing a robotic system to:
  - (a) automatically engage/disengage a mechanical stabilization aid.
  - (b) reposition itself while resolving stiff environmental constraints.
  - (c) manage contact forces and torques while in motion.

6. Climbing Test Overview

The climbing test features a battery-powered, wireless NASA/DARPA Robonaut system (zero-g configuration) mounted on a 380 lb air-bearing sled (Figure 8) for a combined weight exceeding 800 lbs. Floating on an expansive air-bearing floor at NASA's Johnson Space Center, the robot is able to move under its own power by exerting fingertip pressure on a specially built planar climbing mockup representing the outer hull of a spacecraft. The test configuration emulates microgravity in three nearly frictionless degrees-of-freedom (DOFs) required to maneuver between worksites on the mockup.

Fig. 8. Robonaut mounted on an air-bearing sled.

The supine orientation of the robot opens up a huge workspace for its single stabilizing leg, which was exercised extensively during the test. Leg operations in the climbing sequence include stowing/deploying, automated WIF insertion/retraction and constrained leg motions. Force sensors mounted in the forearms and ankle were used to monitor and control contact forces between the robot and the mockup.

During the test, the robot interacts with several climbing mockup features including EVA handrails, a WIF socket and an EVA worksite (Fig. 9). The operational sequence defines an EVR scenario involving each of these elements. A mix of teleoperation and automation is used to complete the sequence. From its starting position, the robot traverses across the mockup using handrails and positions its body for WIF insertion. The latching foot is first aligned by the teleoperator and then automatically inserted with force-moment accommodation (FMA) control until the spring-loaded latches engage. With the robot stabilized in this fashion, the leg is commanded to automatically reposition the upper body under the EVA worksite while resolving the planar constraints imposed by the air-bearing floor. Upon reaching the worksite, the leg is parked to stabilize the robot as it performs a dexterous manipulation task. After the task is complete, the robot retracts its foot out of the WIF socket and climbs away to the next worksite.

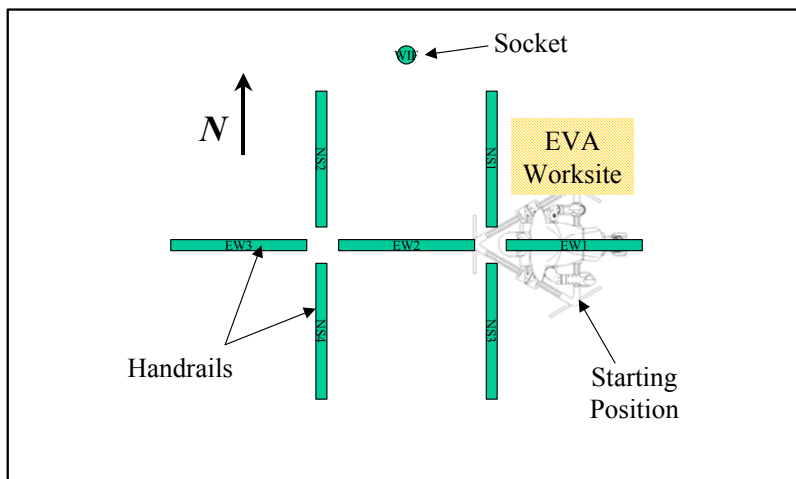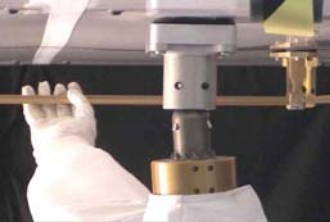Fig. 9. Planar climbing mockup constructed over air-bearing floor.

Fig. 10. Climbing mockup layout (plan view, not to scale).

7. Operational Sequence

Table 1. Experimental test procedure.

1. RMS release 1.1. Robot at starting position (riding RMS - leg stowed and air off). 1.2. Stabilize at handrail EW1. 1.3. RMS release (turn air on).	
2. Translate from EW1 to NS2 2.1. Translate from handrail EW1 to EW2 (head leading). 2.2. Translate from EW2 to NS2. 2.3. Reorient body 90 deg (head pointing S).	
3. Position body for WIF insertion 3.1. Stabilize using handrails EW2 and EW3. 3.2. Deploy leg (automatic move from STOW to SAFE configuration, foot should be visible in teleoperator's helmet-mounted display). 3.3. Adjust body orientation until WIF socket in view and near foot.	

4. WIF insertion
    4.1. Teleoperated alignment: align foot within WIF socket capture envelope (tip occluded, no contact).
    4.2. Activate force-moment accommodation (FMA) on leg.
    4.3. Automatic insertion: drive foot into socket until latches fully engaged (no spline visible around base of foot).	

5. Constrained leg motion
    5.1. Release handrails EW2 and EW3.
    5.2. Activate FMA on leg.
    5.3. Drive leg in constrained planar motion to reposition upper body at EVA worksite.	

6. Stabilized at EVA worksite
    6.1. Attach tether hook to handrail NS1.
    6.2. Brush connector to remove contamination.
    6.3. Unlatch and inspect connector.
    6.4. Reinstall connector.
    6.5. Remove tether hook from handrail NS1.	

7. WIF retraction
    7.1. Stabilize using handrails EW1 and NS1.
    7.2. Activate FMA on leg.
    7.3. Release latches on foot.
    7.4. Automatic retraction: drive foot out of socket until clear.
    7.5. Deactivate FMA on leg.
    7.6. Stow leg (automatic move to STOW configuration).	

8. Translate to next worksite
    8.1. Transition to handrail EW2.
    8.2. Translate from handrail EW2 to EW3 (leg leading).
    8.3. Stabilize at handrail EW3.	

9. Results

The climbing test was performed over a two-week period (1/26/04 - 2/6/04) at the Johnson Space Center. Battery-powered operations were limited to 1.5 hours, nominally reserving about 40% of battery capacity to accommodate variable loading conditions. Umbilical-powered operations were limited in duration by teleoperator fatigue to approximately the same amount of time but could be resumed after a break.

9.1 *Climbing gaits*

Two distinct climbing gaits were successfully employed during the test. The first, more natural-looking gait closely resembles bipedal walking and consists of hand-over-hand motion along a handrail approximately aligned with the spine of the robot. The second gait designates a leading hand and a trailing hand that alternately grasp the handrail to produce motion reminiscent of an inchworm. Average translation speeds of 0.4 in/sec were achieved using both gaits for linear traverses.

Although both hand-over-hand and inchworm gaits necessarily alternate between serial (weak) and parallel (strong) support phases, the inchworm gait never strays far from parallel support and, therefore, offers the ability to stop or change course quickly. This worked well in practice, as the teleoperator was able to maintain control of body orientation even while repositioning the grasp by loosely capturing the handrail at all times.

Average rotation speeds of 3 deg/sec were produced while executing turning maneuvers during the climbing test sequence. To be sure, the fact that the robot was constrained to move in a plane greatly simplified attitude control, as compared to the general unconstrained case of a body in free flight. Techniques such as gyroscopic stabilization may be required to help the spacewalking robot maintain attitude control on orbit.

A variety of climbing maneuvers were successfully attempted during the test. The ability to stabilize the body using the arms was demonstrated in steps 3.1 and 7.1. The ability to control body orientation was critical to steps 2.3, 3.3 and 8.1 of the Operational Sequence. Transitioning from one handrail to the next required a hand-over-hand technique to span the gap, as in steps 2.1 and 8.2.

Certain climbing maneuvers were attempted but ruled infeasible without improvements to the robotic system. For example, side-to-side climbing traverses along a handrail oriented at right angles to the spine of the robot were hampered by the camera field-of-view, which could not encompass both hands at the required separation, and robot wrist joint limits, which reduce the arm workspace.

Unnecessarily large contact forces were observed during teleoperated climbing, partly due to insufficient force feedback through the telepresence interface. Software safety shutdowns were implemented to protect the robot from excessive forces during constrained motions and parallel manipulation phases. These shutdowns, however, interrupted task flow and resulted in degraded performance. Automation can reduce undesirable components of the contact force while improving stance stability but will require sophisticated planning or human assistance in choosing handholds[7].

9.2 *Automated WIF insertion*

The stabilizing leg performed very well during automated sequences but attempts to teleoperate were less precise due to limitations in the human/machine interface (input devices, force displays and available camera views). Nevertheless, the teleoperator was consistently able to align the robot's latching foot within the WIF socket capture envelope (Fig. 11). Once the teleoperator was satisfied with foot alignment, control transitioned to an automatic insertion routine that drove the foot into contact with the socket and adjusted alignment based on measured forces and torques in a force-moment accommodation (FMA) strategy known as damping control.

Fig. 11. (left) Latching foot; (right) WIF socket.

The active component of the insertion command consists of a constant velocity (0.05 in/sec) open-loop trajectory along the longitudinal axis of the probe (+X). Force-moment accommodation is implemented to passively improve alignment of the probe with the socket as it makes contact inside the bore. Lateral offsets of up to 0.5" were easily tolerated without much lateral force buildup due to the compliancy in the robot's dual-handed grasp. Angular misalignments of up to 11.6° were successfully handled by the controller, which, on average, built up a maximum of 27.1 lbs of force and 33.8 in-lbs of torque while driving the foot into the socket.

The results of a typical automated WIF insertion trial are presented in Figs. 12a and 12b, which show data from the same trial. Insertion progress may be divided into four contact phases beginning with the initial human-assisted alignment phase in which the probe and socket are not in contact. Driving the probe forward along X brings the probe into single-point contact with the lip of the socket, generating small contact forces/moments and resulting in lateral alignment of the probe. The single-point contact phase persists for the first 1.5 inches of insertion, during which insertion position errors are small. It ends abruptly when the other side of the probe contacts the bore and forward progress slows in response to dramatically increased forces and moments during the two-point contact phase.
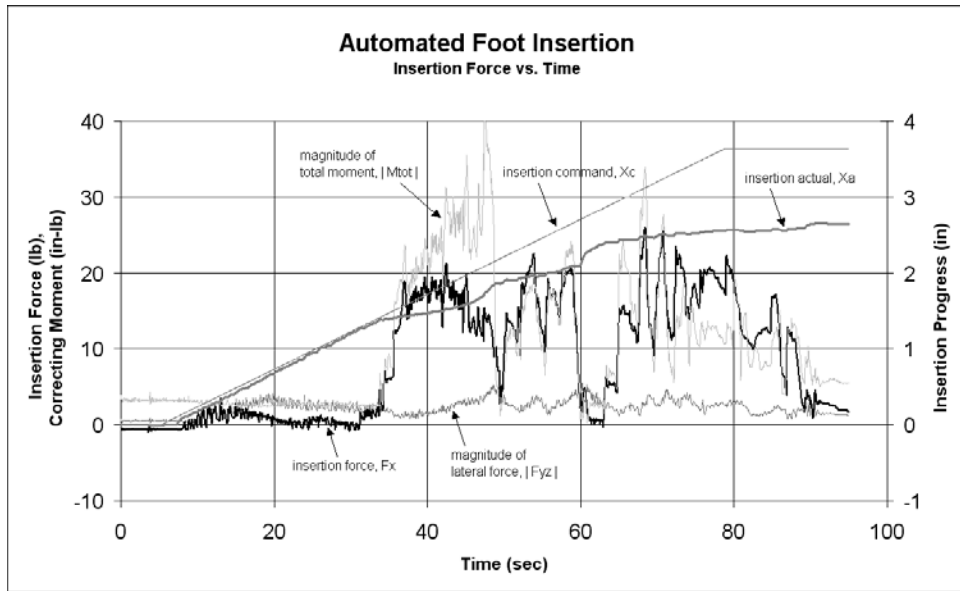
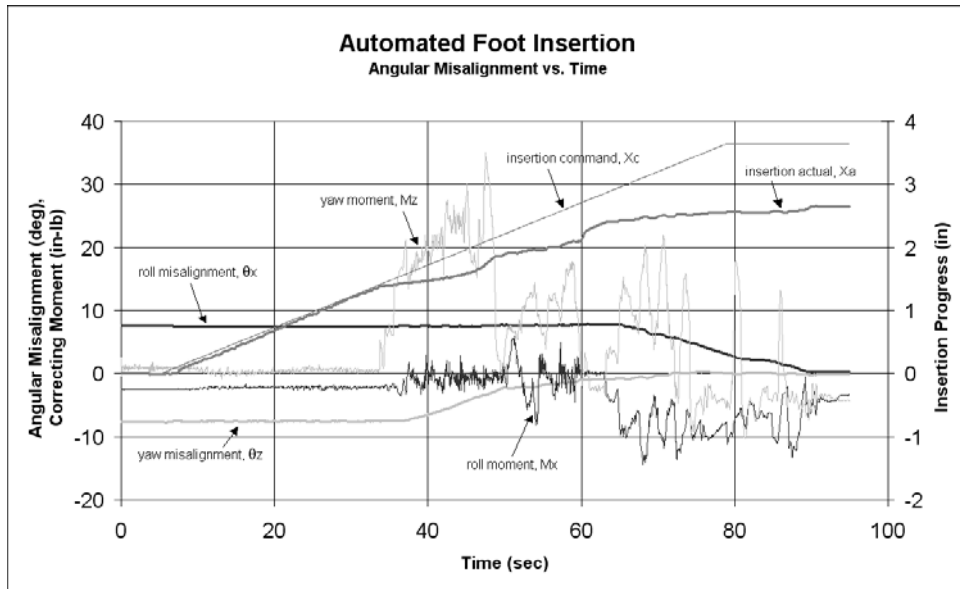Fig. 12a. Insertion force (Fx) recorded during an automated WIF insertion trial.

Fig. 12b. Angular misalignment (θx, θz) recorded during an automated WIF insertion trial.

In order to continue making forward progress into the bore during the two-point contact phase, the probe pitch and yaw misalignments must be corrected in response to pitch and yaw correcting moments (only yaw data is included in Fig. 12b because the pitch data resembles it closely). Roll misalignment, however, is not yet of concern because the probe midbody is symmetrical about the insertion axis. As insertion position error increases, contact forces and moments also grow but the probe gradually rotates into closer alignment with the socket as the controller works to relieve them. During this process, the large error is mitigated by a "slowing" command bias not shown in the plots to avoid excessive correcting motions and forces once the probe slips free. This is precisely what occurs at the 60-second mark, when the forces and moments simultaneously drop off as the probe suddenly unbinds and jumps forward. At this point, the probe is sufficiently well-aligned with the socket to allow unimpeded progress in and out of the bore without building up large forces or moments.

The final step in latching the foot into the WIF socket involves continued progress along +X combined with an axial roll alignment engaging a toothed spline at the base of the foot with a mating pattern inside the lip of the socket (Fig. 11). This step occurs in the last 0.375 inches of travel, as the spline and mating pattern mesh in a multi-point contact phase, and requires almost no pitch or yaw alignments. The mesh geometry limits roll misalignment to 15° but a slight initial angular velocity about the foot axis of symmetry may be needed to overcome binding should the opposing peaks come into contact.

Typically, insertions were completed in 80 seconds or less from start to finish. Maximum forces experienced will be higher for larger initial misalignments and faster insertion speeds and lower for more aggressive FMA gains, until a stability limit is reached. Controller gains were chosen by trial and error to provide stable performance for the .05 ips insertion speed, which was slow enough to let the integral controller align the lateral and rotational axes without building large contact forces.

It is noteworthy that the WIF interface was neither designed nor intended for robotic insertion, but for astronauts who could "feel" their way into and out of the mechanical connection. Even when mated and latched, the interface has noticeable play with generous clearances designed to account for thermal expansion/contraction of the mating parts. The force controller was, nevertheless, able to automatically resolve substantial misalignments while driving the foot all the way in to latch engagement from various starting positions outside the socket.

9.3 *Constrained leg motion*

With the foot latched into the WIF socket, the leg was used to reposition the upper body and stabilize the robot at the worksite. The controller was configured to comply with constraint forces (normal to the air-bearing floor) and moments (parallel to the plane of the floor) at the socket during constrained leg motions. Utilizing a Cartesian roll angular rate command about the WIF socket's axis of symmetry (X-axis), the repositioning maneuver was performed at speeds up to 1.1° per second, resulting in upper body speeds of 0.7" per second measured at the center of the chest 36" away and a cumulative rotation exceeding 60°.

The constrained leg motion data presented in Fig. 13 shows smooth and steady progress in moving the large system inertia about the roll axis as a result of discrete

angular impulses as large as 30 in-lbs. The fact that only positive roll moments were observed whether the robot was accelerating or decelerating suggests that friction cannot be entirely neglected, despite the air-bearing test equipment. Forces and residual moments not related to the desired motion are kept low, effectively resolving the planar constraint of moving across the air-bearing floor.
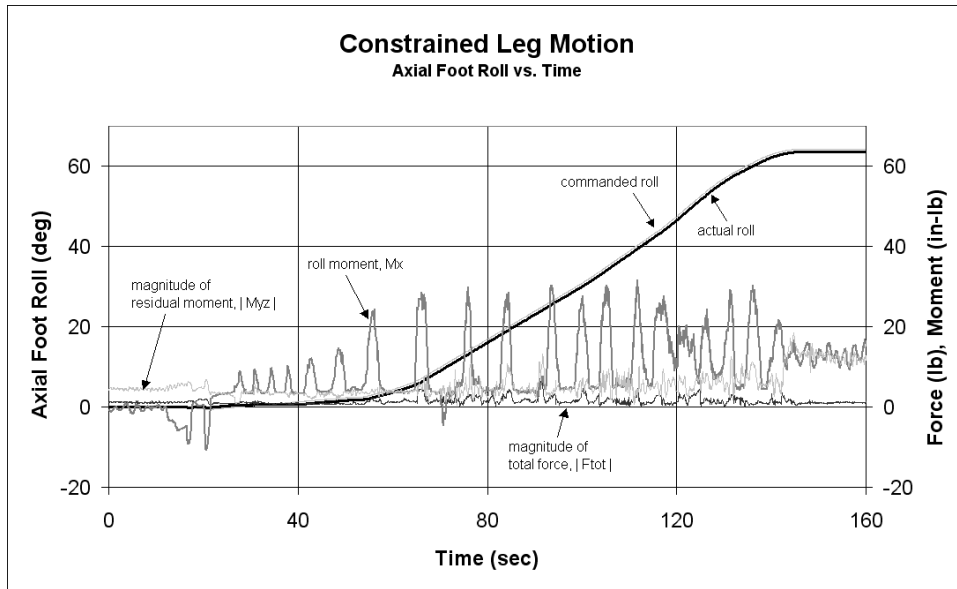

Fig. 13. Constrained leg motion used to reposition the upper body.

10. Conclusion

Over the course of the two-week climbing test, several critical components of robotic spacewalking were demonstrated. These include translating between EVA worksites, stabilizing at a worksite and repositioning/working while stabilized. For the sake of simplicity, EVA tether management was not incorporated into the test procedure except in a single instance at the EVA worksite. Also interesting is the possibility of translating while carrying an object.

The climbing test should be understood as part of a continuing effort to study the particular challenges of deploying robotic systems in space environments designed for humans. At the same time, these experiments test the limits of robotics and teleoperation, demonstrating new EVR capabilities and the feasibility of performing more tasks telerobotically. These limits can be pushed back even further or overcome altogether by introducing appropriate levels of automation where time delay, task dynamics, camera views, force feedback and other factors dominate the results.

Climbing is not the only mode of EVR locomotion available to Robonaut. Other options include riding the RMS, flying with a Simplified Aid for EVA Rescue (SAFER) jetpack and rolling along the ISS Mobile Transporter (MT) rail. These alternate means

complement, but do not replace, the robot's ability to access EVA worksites and transport payloads on its own.

Acknowledgements

References

1. Extravehicular Activity (EVA) Standard Interface Control Document: International Space Station Program Internal Document (SSP 30256), NASA/Johnson Space Center, Houston, Texas, June 1999.
2. Akin, D., Roberts, B., Pilotte, K. and Baker, M., "Robotic Augmentation of EVA for Hubble Telescope Servicing," Proceedings of AIAA Space 2003, Long Beach, CA, September 2003.
3. Rehnmark, F., Currie, N., Ambrose, R.O. and Culbert, C., "Human-Centric Teaming in a Multi-Agent EVA Assembly Task," Proceedings of SAE International Conference on Environmental Systems, Colorado Springs, Colorado, July 2004.
4. Ambrose, R. O., Culbert, C. and Rehnmark, F., "An Experimental Investigation of Dexterous Robots working with EVA Hardware," Proceedings of AIAA Space 2001, Albuquerque, NM, 2001.
5. Ambrose, R. O., et al., "ROBONAUT: NASA's Space Humanoid," IEEE Intelligent Systems Journal, August 2000.
6. Aldridge, H., Bluethmann, W., Ambrose, R. O. and Diftler, M., "Control Architecture for the Robonaut Space Humanoid," Proceedings of the First IEEE-RAS International Conference on Humanoid Robots (Humanoids 2000), Cambridge, Massachusetts, September 2000.
7. Bretl, T., Latombe, J.C. and Rock, S., "Toward Autonomous Free-Climbing Robots," Proceedings of the International Symposium of Robotics Research (ISRR), Siena, Italy, October 2003.

Fredrik Rehnmark is a senior engineer working for Lockheed Martin at NASA's Johnson Space Center and is currently the body design lead on the Robonaut project. His research interests include human augmentation and anthropomorphic robots. He earned an MS in Mechanical Engineering from the University of California at Berkeley. He may be reached at rehnmark@jsc.nasa.gov.

William Bluethmann works for NASA at the Johnson Space Center in the Flight Robotic Systems Branch and currently is the software lead for the Robonaut project. His research interests include manipulator control, force control, distributed autonomy, and task level automation. He earned a Ph.D. in Mechanical Engineering from the University of Kansas. Contact: bluethmann@jsc.nasa.gov.

Ivan Spain is a senior engineer working for Lockheed Martin at NASA's Johnson Space Center and is currently the assistant software lead on the Robonaut project. He earned a BS in Electrical Engineering from Mississippi State University. He may be reached at ivan.m.spain1@jsc.nasa.gov.

Ken Alder is a controls specialist working on the Robonaut controllers for Hernandez Engineering, Inc. at NASA Johnson Space Center. He has a BSME degree from Texas A&M. Contact: ken.alder@jsc.nasa.gov.

S. Michael Goza received his B.S. in Aerospace and Ocean Engineering from Virginia Polytechnique Institute and State University in 1984. From 1980 to the present he has worked at the National Aeronautics and Space Administration Johnson Space Center (NASA-JSC) on a number of projects ranging from aerodynamic analysis, to computer graphics, to robotics. Currently, S. Michael Goza is part of the Robonaut team in charge of telepresence control software, human – machine interfaces, mobile platform integration, and computer simulation.

Robert O. Ambrose received his B.S. and M.S. in Mechanical Engineering from Washington University in St. Louis, and his Ph.D. from the University of Texas at Austin. His publications include topics in robot design, space environmental modeling, actuator development, kinematics, kinetics, bio-mechanics, interactive design software and non-linear optimism. He has built robotic systems for space, microelectronics, nuclear and agricultural applications. Systems that he has designed include multiple manipulators, force feedback joysticks, gantries, walking machines and wheeled robots. He is currently employed at NASA's Johnson Space Center, where he serves as the Robonaut Project Leader. Contact: Robert.Ambrose@jsc.nasa.gov